A Joint Fermi-GBM and LIGO/Virgo Analysis of Compact Binary Mergers from the First and Second Gravitational-wave Observing Runs

R. Hamburg[1,2], C. Fletcher[3], E. Burns[4,212], A. Goldstein[3], E. Bissaldi[5,6], M. S. Briggs[1,2], W. H. Cleveland[3], M. M. Giles[7],
C. M. Hui[8], D. Kocevski[8], S. Lesage[1,2], B. Mailyan[2], C. Malacaria[3,8,212], S. Poolakkil[1,2], R. Preece[1], O. J. Roberts[3],
P. Veres[2], A. von Kienlin[9], C. A. Wilson-Hodge[8], J. Wood[10,212]
Fermi Gamma-Ray Burst Monitor,
and
R. Abbott[11], T. D. Abbott[12], S. Abraham[13], F. Acernese[14,15], K. Ackley[16], C. Adams[17], R. X. Adhikari[11], V. B. Adya[18],
C. Affeldt[19,20], M. Agathos[21,22], K. Agatsuma[23], N. Aggarwal[24], O. D. Aguiar[25], A. Aich[26], L. Aiello[27,28], A. Ain[13], P. Ajith[29],
G. Allen[30], A. Allocca[31], P. A. Altin[18], A. Amato[32], S. Anand[11], A. Ananyeva[11], S. B. Anderson[11], W. G. Anderson[33],
S. V. Angelova[34], S. Ansoldi[35,36], S. Antier[37], S. Appert[11], K. Arai[11], M. C. Araya[11], J. S. Areeda[38], M. Arène[37], N. Arnaud[39,40],
S. M. Aronson[41], S. Ascenzi[27,42], G. Ashton[16], S. M. Aston[17], P. Astone[43], F. Aubin[44], P. Aufmuth[20], K. AultONeal[45], C. Austin[12],
V. Avendano[46], S. Babak[37], P. Bacon[37], F. Badaracco[27,28], M. K. M. Bader[47], S. Bae[48], A. M. Baer[49], J. Baird[37], F. Baldaccini[50,51],
G. Ballardin[40], S. W. Ballmer[52], A. Bals[45], A. Balsamo[49], G. Baltus[53], S. Banagiri[54], D. Bankar[13], R. S. Bankar[13],
J. C. Barayoga[11], C. Barbieri[55,56], B. C. Barish[11], D. Barker[57], K. Barkett[58], P. Barneo[59], F. Barone[15,60], B. Barr[61], L. Barsotti[62],
M. Barsuglia[37], D. Barta[63], J. Bartlett[57], I. Bartos[41], R. Bassiri[64], A. Basti[31,65], M. Bawaj[51,66], J. C. Bayley[61], M. Bazzan[67,68],
B. Bécsy[69], M. Bejger[70], I. Belahcene[39], A. S. Bell[61], D. Beniwal[71], M. G. Benjamin[45], J. D. Bentley[23], F. Bergamin[19],
B. K. Berger[64], G. Bergmann[19,20], S. Bernuzzi[21], C. P. L. Berry[24], D. Bersanetti[72], A. Bertolini[47], J. Betzwieser[17], R. Bhandare[73],
A. V. Bhandari[13], J. Bidler[38], E. Biggs[33], I. A. Bilenko[74], G. Billingsley[11], R. Birney[75], O. Birnholtz[76,77], S. Biscans[11,62],
M. Bischi[78,79], S. Biscoveanu[62], A. Bisht[20], G. Bissenbayeva[26], M. Bitossi[31,40], M. A. Bizouard[80], J. K. Blackburn[11],
J. Blackman[58], C. D. Blair[17], D. G. Blair[81], R. M. Blair[57], F. Bobba[82,83], N. Bode[19,20], M. Boer[80], Y. Boetzel[84], G. Bogaert[80],
F. Bondu[85], E. Bonilla[64], R. Bonnand[44], P. Booker[19,20], B. A. Boom[47], V. Boschi[31], S. Bose[13], V. Bossilkov[81],
J. Bosveld[81], Y. Bouffanais[67,68], A. Bozzi[40], C. Bradaschia[31], P. R. Brady[33], A. Bramley[17], M. Branchesi[27,28], J. E. Brau[86],
M. Breschi[21], T. Briant[87], J. H. Briggs[61], F. Brighenti[78,79], A. Brillet[80], M. Brinkmann[19,20], P. Brockill[33], A. F. Brooks[11],
J. Brooks[40], D. D. Brown[71], S. Brunett[11], G. Bruno[88], R. Bruntz[49], A. Buikema[62], T. Bulik[89], H. J. Bulten[47,90], A. Buonanno[91,92],
D. Buskulic[44], R. L. Byer[64], M. Cabero[19,20], L. Cadonati[93], G. Cagnoli[94], C. Cahillane[11], J. Calderón Bustillo[16], J. D. Callaghan[61],
T. A. Callister[11], E. Calloni[15,95], J. B. Camp[4], M. Canepa[72,96], K. C. Cannon[97], H. Cao[71], J. Cao[98], G. Carapella[82,83],
F. Carbognani[40], S. Caride[99], M. F. Carney[24], G. Carullo[31,65], J. Casanueva Diaz[31], C. Casentini[42,100], J. Castañeda[59],
S. Caudill[47], M. Cavaglià[101], F. Cavalier[39], R. Cavalieri[40], G. Cella[31], P. Cerdá-Durán[102], E. Cesarini[42,103], O. Chaibi[80],
K. Chakravarti[13], C. Chan[97], M. Chan[61], S. Chao[104], P. Charlton[105], E. A. Chase[24], E. Chassande-Mottin[37], D. Chatterjee[33],
M. Chaturvedi[73], H. Y. Chen[106], X. Chen[81], Y. Chen[58], H.-P. Cheng[41], C. K. Cheong[107], H. Y. Chia[41], F. Chiadini[83,108],
R. Chierici[109], A. Chincarini[72], A. Chiummo[40], G. Cho[110], H. S. Cho[111], M. Cho[92], N. Christensen[80], Q. Chu[81], S. Chua[87],
K. W. Chung[107], S. Chung[81], G. Ciani[67,68], P. Ciecielag[70], M. Cieślar[70], A. A. Ciobanu[71], R. Ciolfi[68,112], F. Cipriano[80],
A. Cirone[72,96], F. Clara[57], J. A. Clark[93], P. Clearwater[113], S. Clesse[88], F. Cleva[80], E. Coccia[27,28], P.-F. Cohadon[87], D. Cohen[39],
M. Colleoni[114], C. G. Collette[115], C. Collins[23], M. Colpi[55,56], M. Constancio, Jr.[25], L. Conti[68], S. J. Cooper[23], P. Corban[17],
T. R. Corbitt[12], I. Cordero-Carrión[116], S. Corezzi[50,51], K. R. Corley[117], N. Cornish[69], D. Corre[39], A. Corsi[99], S. Cortese[40],
C. A. Costa[25], R. Cotesta[91], M. W. Coughlin[11], S. B. Coughlin[24,118], J.-P. Coulon[80], S. T. Countryman[117], P. Couvares[11],
P. B. Covas[114], D. M. Coward[81], M. J. Cowart[17], D. C. Coyne[11], R. Coyne[119], J. D. E. Creighton[33], T. D. Creighton[26], J. Cripe[12],
M. Croquette[87], S. G. Crowder[120], J.-R. Cudell[53], T. J. Cullen[12], A. Cumming[61], R. Cummings[61], L. Cunningham[61], E. Cuoco[40],
M. Curylo[89], T. Dal Canton[91], G. Dálya[121], A. Dana[64], L. M. Daneshgaran-Bajastani[122], B. D'Angelo[72,96], S. L. Danilishin[19,20],
S. D'Antonio[42], K. Danzmann[19,20], C. Darsow-Fromm[123], A. Dasgupta[124], L. E. H. Datrier[61], V. Dattilo[40], I. Dave[73], M. Davier[39],
G. S. Davies[125], D. Davis[52], E. J. Daw[126], D. DeBra[64], M. Deenadayalan[13], J. Degallaix[32], M. De Laurentis[15,95], S. Deléglise[87],
M. Delfavero[76], N. De Lillo[61], W. Del Pozzo[31,65], L. M. DeMarchi[24], V. D'Emilio[118], N. Demos[62], T. Dent[125],
R. De Pietri[127,128], R. De Rosa[15,95], C. De Rossi[40], R. DeSalvo[129], O. de Varona[19,20], S. Dhurandhar[13], M. C. Díaz[26],
M. Diaz-Ortiz, Jr.[41], T. Dietrich[47], L. Di Fiore[15], C. Di Fronzo[23], C. Di Giorgio[82,83], F. Di Giovanni[102], M. Di Giovanni[130,131],
T. Di Girolamo[15,95], A. Di Lieto[31,65], B. Ding[115], S. Di Pace[43,132], I. Di Palma[43,132], F. Di Renzo[31,65], A. K. Divakarla[41],
A. Dmitriev[23], Z. Doctor[106], F. Donovan[62], K. L. Dooley[118], S. Doravari[13], I. Dorrington[118], T. P. Downes[33], M. Drago[27,28],
J. C. Driggers[57], Z. Du[98], J.-G. Ducoin[39], P. Dupej[61], O. Durante[82,83], D. D'Urso[133,134], S. E. Dwyer[57], P. J. Easter[16], G. Eddolls[61],
B. Edelman[86], T. B. Edo[126], O. Edy[135], A. Effler[17], P. Ehrens[11], J. Eichholz[18], S. S. Eikenberry[41], M. Eisenmann[44],
R. A. Eisenstein[62], A. Ejlli[118], L. Errico[15,95], R. C. Essick[106], H. Estelles[114], D. Estevez[44], Z. B. Etienne[136], T. Etzel[11], M. Evans[62],
T. M. Evans[17], B. E. Ewing[137], V. Fafone[27,42,100], S. Fairhurst[118], X. Fan[98], S. Farinon[72], B. Farr[86], W. M. Farr[138,139],
E. J. Fauchon-Jones[118], M. Favata[46], M. Fays[126], M. Fazio[140], J. Feicht[11], M. M. Fejer[64], F. Feng[37], E. Fenyvesi[63,141],
D. L. Ferguson[93], A. Fernandez-Galiana[62], I. Ferrante[31,65], E. C. Ferreira[25], T. A. Ferreira[25], F. Fidecaro[31,65], I. Fiori[40],
D. Fiorucci[27,28], M. Fishbach[106], R. P. Fisher[49], R. Fittipaldi[83,142], M. Fitz-Axen[54], V. Fiumara[83,143], R. Flaminio[44,144],

E. Floden[54], E. Flynn[38], H. Fong[97], J. A. Font[102,145], P. W. F. Forsyth[18], J.-D. Fournier[80], S. Frasca[43,132], F. Frasconi[31], Z. Frei[121], A. Freise[23], R. Frey[86], V. Frey[39], P. Fritschel[62], V. V. Frolov[17], G. Fronzè[146], P. Fulda[41], M. Fyffe[17], H. A. Gabbard[61], B. U. Gadre[91], S. M. Gaebel[23], J. R. Gair[91], S. Galaudage[16], D. Ganapathy[62], S. G. Gaonkar[13], C. García-Quirós[114], F. Garufi[15,95], B. Gateley[57], S. Gaudio[45], V. Gayathri[147], G. Gemme[72], E. Genin[40], A. Gennai[31], D. George[30], J. George[73], L. Gergely[148], S. Ghonge[93], Abhirup Ghosh[91], Archisman Ghosh[47,149,150,151], S. Ghosh[33], B. Giacomazzo[130,131], J. A. Giaime[12,17], K. D. Giardina[17], D. R. Gibson[75], C. Gier[34], K. Gill[117], J. Glanzer[12], J. Gniesmer[123], P. Godwin[137], E. Goetz[12,101], R. Goetz[41], N. Gohlke[19,20], B. Goncharov[16], G. González[12], A. Gopakumar[152], S. E. Gossan[11], M. Gosselin[31,40,65], R. Gouaty[44], B. Grace[18], A. Grado[15,153], M. Granata[32], A. Grant[61], S. Gras[62], P. Grassia[11], C. Gray[57], R. Gray[61], G. Greco[78,79], A. C. Green[41], R. Green[118], E. M. Gretarsson[45], H. L. Griggs[93], G. Grignani[50,51], A. Grimaldi[130,131], S. J. Grimm[27,28], H. Grote[118], S. Grunewald[91], P. Gruning[39], G. M. Guidi[78,79], A. R. Guimaraes[12], G. Guixé[59], H. K. Gulati[124], Y. Guo[47], A. Gupta[137], Anchal Gupta[11], P. Gupta[47], E. K. Gustafson[11], R. Gustafson[154], L. Haegel[114], O. Halim[27,28], E. D. Hall[62], E. Z. Hamilton[118], G. Hammond[61], M. Haney[84], M. M. Hanke[19,20], J. Hanks[57], C. Hanna[137], M. D. Hannam[118], O. A. Hannuksela[107], T. J. Hansen[45], J. Hanson[17], T. Harder[80], T. Hardwick[12], K. Haris[29], J. Harms[27,28], G. M. Harry[155], I. W. Harry[135], R. K. Hasskew[17], C.-J. Haster[62], K. Haughian[61], F. J. Hayes[61], J. Healy[76], A. Heidmann[87], M. C. Heintze[17], J. Heinze[19,20], H. Heitmann[80], F. Hellman[156], P. Hello[39], G. Hemming[40], M. Hendry[61], I. S. Heng[61], E. Hennes[47], J. Hennig[19,20], M. Heurs[19,20], S. Hild[61,157], T. Hinderer[47,149,151], S. Y. Hoback[38,155], S. Hochheim[19,20], E. Hofgard[64], D. Hofman[32], A. M. Holgado[30], N. A. Holland[18], K. Holt[17], D. E. Holz[106], P. Hopkins[118], C. Horst[33], J. Hough[61], E. J. Howell[81], C. G. Hoy[118], Y. Huang[62], M. T. Hübner[16], E. A. Huerta[30], D. Huet[39], B. Hughey[45], V. Hui[44], S. Husa[114], S. H. Huttner[61], R. Huxford[137], T. Huynh-Dinh[17], B. Idzkowski[89], A. Iess[42,100], H. Inchauspe[41], C. Ingram[71], G. Intini[43,132], J.-M. Isac[87], M. Isi[62], B. R. Iyer[29], T. Jacqmin[87], S. J. Jadhav[158], S. P. Jadhav[13], A. L. James[118], K. Jani[93], N. N. Janthalur[158], P. Jaranowski[159], D. Jariwala[41], R. Jaume[114], A. C. Jenkins[160], J. Jiang[41], G. R. Johns[49], A. W. Jones[23], D. I. Jones[161], J. D. Jones[57], P. Jones[23], R. Jones[61], R. J. G. Jonker[47], L. Ju[81], J. Junker[19,20], C. V. Kalaghatgi[118], V. Kalogera[24], B. Kamai[11], S. Kandhasamy[13], G. Kang[48], J. B. Kanner[11], S. J. Kapadia[29], S. Karki[86], R. Kashyap[29], M. Kasprzack[11], W. Kastaun[19,20], S. Katsanevas[40], E. Katsavounidis[62], W. Katzman[17], S. Kaufer[20], K. Kawabe[57], F. Kéfélian[80], D. Keitel[135], A. Keivani[117], R. Kennedy[126], J. S. Key[162], S. Khadka[64], F. Y. Khalili[74], I. Khan[27,42], S. Khan[19,20], Z. A. Khan[98], E. A. Khazanov[163], N. Khetan[27,28], M. Khursheed[73], N. Kijbunchoo[18], Chunglee Kim[164], G. J. Kim[93], J. C. Kim[165], K. Kim[107], W. Kim[71], W. S. Kim[166], Y.-M. Kim[167], C. Kimball[24], P. J. King[57], M. Kinley-Hanlon[61], R. Kirchhoff[19,20], J. S. Kissel[57], L. Kleybolte[123], S. Klimenko[41], T. D. Knowles[136], P. Koch[19,20], S. M. Koehlenbeck[19,20], G. Koekoek[47,157], S. Koley[47], V. Kondrashov[11], A. Kontos[168], N. Koper[19,20], M. Korobko[123], W. Z. Korth[11], M. Kovalam[81], D. B. Kozak[11], V. Kringel[19,20], N. V. Krishnendu[169], A. Królak[170,171], N. Krupinski[33], G. Kuehn[19,20], A. Kumar[158], P. Kumar[172], Rahul Kumar[57], Rakesh Kumar[124], S. Kumar[29], L. Kuo[104], A. Kutynia[170], B. D. Lackey[91], D. Laghi[31,65], E. Lalande[173], T. L. Lam[107], A. Lamberts[80,174], M. Landry[57], B. B. Lane[62], R. N. Lang[175], J. Lange[76], B. Lantz[64], R. K. Lanza[62], I. La Rosa[44], A. Lartaux-Vollard[39], P. D. Lasky[16], M. Laxen[17], A. Lazzarini[11], C. Lazzaro[68], P. Leaci[43,132], S. Leavey[19,20], Y. K. Lecoeuche[57], C. H. Lee[111], H. M. Lee[176], H. W. Lee[165], J. Lee[110], K. Lee[64], J. Lehmann[19,20], N. Leroy[39], N. Letendre[44], Y. Levin[16], A. K. Y. Li[107], J. Li[98], K. li[107], T. G. F. Li[107], X. Li[58], F. Linde[47,177], S. D. Linker[122], J. N. Linley[61], T. B. Littenberg[178], J. Liu[19,20], X. Liu[33], M. Llorens-Monteagudo[102], R. K. L. Lo[11], A. Lockwood[179], L. T. London[62], A. Longo[180,181], M. Lorenzini[27,28], V. Loriette[182], M. Lormand[17], G. Losurdo[31], J. D. Lough[19,20], C. O. Lousto[76], G. Lovelace[38], H. Lück[19,20], D. Lumaca[42,100], A. P. Lundgren[135], Y. Ma[58], R. Macas[118], S. Macfoy[34], M. MacInnis[62], D. M. Macleod[118], I. A. O. MacMillan[155], A. Macquet[80], I. Magaña Hernandez[33], F. Magaña-Sandoval[41], R. M. Magee[137], E. Majorana[43], I. Maksimovic[182], A. Malik[73], N. Man[80], V. Mandic[54], V. Mangano[43,61,132], G. L. Mansell[57,62], M. Manske[33], M. Mantovani[40], M. Mapelli[67,68], F. Marchesoni[51,66,183], F. Marion[44], S. Márka[117], Z. Márka[117], C. Markakis[22], A. S. Markosyan[64], A. Markowitz[11], E. Maros[11], A. Marquina[116], S. Marsat[37], F. Martelli[78,79], I. W. Martin[61], R. M. Martin[46], V. Martinez[94], D. V. Martynov[23], H. Masalehdan[123], K. Mason[62], E. Massera[126], A. Masserot[44], T. J. Massinger[62], M. Masso-Reid[61], S. Mastrogiovanni[37], A. Matas[91], F. Matichard[11,62], N. Mavalvala[62], E. Maynard[12], J. J. McCann[81], R. McCarthy[57], D. E. McClelland[18], S. McCormick[17], L. McCuller[62], S. C. McGuire[184], C. McIsaac[135], J. McIver[11], D. J. McManus[18], T. McRae[18], S. T. McWilliams[136], D. Meacher[33], G. D. Meadors[16], M. Mehmet[19,20], A. K. Mehta[29], E. Mejuto Villa[83,129], A. Melatos[113], G. Mendell[57], R. A. Mercer[33], L. Mereni[32], K. Merfeld[86], E. L. Merilh[57], J. D. Merritt[86], M. Merzougui[80], S. Meshkov[11], C. Messenger[61], C. Messick[185], R. Metzdorff[87], P. M. Meyers[113], F. Meylahn[19,20], A. Mhaske[13], A. Miani[130,131], H. Miao[23], I. Michaloliakos[41], C. Michel[32], H. Middleton[113], L. Milano[15,95], A. L. Miller[41,43,132], M. Millhouse[113], J. C. Mills[118], E. Milotti[36,186], M. C. Milovich-Goff[122], O. Minazzoli[80,187], Y. Minenkov[42], A. Mishkin[41], C. Mishra[188], T. Mistry[126], S. Mitra[13], V. P. Mitrofanov[74], G. Mitselmakher[41], R. Mittleman[62], G. Mo[62], K. Mogushi[101], S. R. P. Mohapatra[62], S. R. Mohite[33], M. Molina-Ruiz[156], M. Mondin[122], M. Montani[78,79], C. J. Moore[23], D. Moraru[57], F. Morawski[70], G. Moreno[57], S. Morisaki[97], B. Mours[189], C. M. Mow-Lowry[23], S. Mozzon[135], F. Muciaccia[43,132], Arunava Mukherjee[61], D. Mukherjee[137], S. Mukherjee[26], Subroto Mukherjee[124], N. Mukund[19,20], A. Mullavey[17], J. Munch[71], E. A. Muñiz[52], P. G. Murray[61], A. Nagar[103,146,190], I. Nardecchia[42,100], L. Naticchioni[43,132], R. K. Nayak[191], B. F. Neil[81], J. Neilson[83,129], G. Nelemans[47,192], T. J. N. Nelson[17], M. Nery[19,20], A. Neunzert[154], K. Y. Ng[62], S. Ng[71], C. Nguyen[37], P. Nguyen[86], D. Nichols[47,151], S. A. Nichols[12], S. Nissanke[47,151], F. Nocera[40], M. Noh[62], C. North[118], D. Nothard[193], L. K. Nuttall[135], J. Oberling[57], B. D. O'Brien[41], G. Oganesyan[27,28], G. H. Ogin[194], J. J. Oh[166], S. H. Oh[166], F. Ohme[19,20], H. Ohta[97], M. A. Okada[25], M. Oliver[114], C. Olivetto[40], P. Oppermann[19,20], Richard J. Oram[17], B. O'Reilly[17], R. G. Ormiston[54], L. F. Ortega[41],

R. O'Shaughnessy[76], S. Ossokine[91], C. Osthelder[11], D. J. Ottaway[71], H. Overmier[17], B. J. Owen[99], A. E. Pace[137], G. Pagano[31,65], M. A. Page[81], G. Pagliaroli[27,28], A. Pai[147], S. A. Pai[73], J. R. Palamos[86], O. Palashov[163], C. Palomba[43], H. Pan[104], P. K. Panda[158], P. T. H. Pang[47], C. Pankow[24], F. Pannarale[43,132], B. C. Pant[73], F. Paoletti[31], A. Paoli[40], A. Parida[13], W. Parker[17,184], D. Pascucci[47,61], A. Pasqualetti[40], R. Passaquieti[31,65], D. Passuello[31], B. Patricelli[31,65], E. Payne[16], B. L. Pearlstone[61], T. C. Pechsiri[41], A. J. Pedersen[52], M. Pedraza[11], A. Pele[17], S. Penn[195], A. Perego[130,131], C. J. Perez[57], C. Périgois[44], A. Perreca[130,131], S. Perriès[109], J. Petermann[123], H. P. Pfeiffer[91], M. Phelps[19,20], K. S. Phukon[13,47,177], O. J. Piccinni[43,132], M. Pichot[80], M. Piendibene[31,65], F. Piergiovanni[78,79], V. Pierro[83,129], G. Pillant[40], L. Pinard[32], I. M. Pinto[83,103,129], K. Piotrzkowski[88], M. Pirello[57], M. Pitkin[196], W. Plastino[180,181], R. Poggiani[31,65], D. Y. T. Pong[107], S. Ponrathnam[13], P. Popolizio[40], E. K. Porter[37], J. Powell[197], A. K. Prajapati[124], K. Prasai[64], R. Prasanna[158], G. Pratten[23], T. Prestegard[33], M. Principe[83,103,129], G. A. Prodi[130,131], L. Prokhorov[23], M. Punturo[51], P. Puppo[43], M. Pürrer[91], H. Qi[118], V. Quetschke[26], P. J. Quinonez[45], F. J. Raab[57], G. Raaijmakers[47,151], H. Radkins[57], N. Radulesco[80], P. Raffai[121], H. Rafferty[198], S. Raja[73], C. Rajan[73], B. Rajbhandari[99], M. Rakhmanov[26], K. E. Ramirez[26], A. Ramos-Buades[114], Javed Rana[13], K. Rao[24], P. Rapagnani[43,132], V. Raymond[118], M. Razzano[31,65], J. Read[38], T. Regimbau[44], L. Rei[72], S. Reid[34], D. H. Reitze[11,41], P. Rettegno[146,199], F. Ricci[43,132], C. J. Richardson[45], J. W. Richardson[11], P. M. Ricker[30], G. Riemenschneider[146,199], K. Riles[154], M. Rizzo[24], N. A. Robertson[11,61], F. Robinet[39], A. Rocchi[42], R. D. Rodriguez-Soto[45], L. Rolland[44], J. G. Rollins[11], V. J. Roma[86], M. Romanelli[85], R. Romano[14,15], C. L. Romel[57], I. M. Romero-Shaw[16], J. H. Romie[17], C. A. Rose[33], D. Rose[38], K. Rose[193], D. Rosińska[89], S. G. Rosofsky[30], M. P. Ross[179], S. Rowan[61], S. J. Rowlinson[23], P. K. Roy[26], Santosh Roy[13], Soumen Roy[200], P. Ruggi[40], G. Rutins[75], K. Ryan[57], S. Sachdev[137], T. Sadecki[57], M. Sakellariadou[160], O. S. Salafia[55,56,201], L. Salconi[40], M. Saleem[169], A. Samajdar[47], E. J. Sanchez[11], L. E. Sanchez[11], N. Sanchis-Gual[202], J. R. Sanders[203], K. A. Santiago[46], E. Santos[80], N. Sarin[16], B. Sassolas[32], B. S. Sathyaprakash[118,137], O. Sauter[44], R. L. Savage[57], V. Savant[13], D. Sawant[147], S. Sayah[32], D. Schaetzl[11], P. Schale[86], M. Scheel[58], J. Scheuer[24], P. Schmidt[23], R. Schnabel[123], R. M. S. Schofield[86], A. Schönbeck[123], E. Schreiber[19,20], B. W. Schulte[19,20], B. F. Schutz[118], O. Schwarm[194], E. Schwartz[17], J. Scott[61], S. M. Scott[18], E. Seidel[30], D. Sellers[17], A. S. Sengupta[200], N. Sennett[91], D. Sentenac[40], V. Sequino[72], A. Sergeev[163], Y. Setyawati[19,20], D. A. Shaddock[18], T. Shaffer[57], M. S. Shahriar[24], A. Sharma[27,28], P. Sharma[73], P. Shawhan[92], H. Shen[30], M. Shikauchi[97], R. Shink[173], D. H. Shoemaker[62], D. M. Shoemaker[93], K. Shukla[156], S. ShyamSundar[73], K. Siellez[93], M. Sieniawska[70], D. Sigg[57], L. P. Singer[4], D. Singh[137], N. Singh[89], A. Singha[61], A. Singhal[27,43], A. M. Sintes[114], V. Sipala[133,134], V. Skliris[118], B. J. J. Slagmolen[18], T. J. Slaven-Blair[81], J. Smetana[23], J. R. Smith[38], R. J. E. Smith[16], S. Somala[204], E. J. Son[166], S. Soni[12], B. Sorazu[61], V. Sordini[109], F. Sorrentino[72], T. Souradeep[13], E. Sowell[99], A. P. Spencer[61], M. Spera[67,68], A. K. Srivastava[124], V. Srivastava[52], K. Staats[24], C. Stachie[80], M. Standke[19,20], D. A. Steer[37], M. Steinke[19,20], J. Steinlechner[61,123], S. Steinlechner[123], D. Steinmeyer[19,20], D. Stocks[64], D. J. Stops[23], M. Stover[193], K. A. Strain[61], G. Stratta[79,205], A. Strunk[57], R. Sturani[206], A. L. Stuver[207], S. Sudhagar[13], V. Sudhir[62], T. Z. Summerscales[208], L. Sun[11], S. Sunil[124], A. Sur[70], J. Suresh[97], P. J. Sutton[118], B. L. Swinkels[47], M. J. Szczepańczyk[41], M. Tacca[47], S. C. Tait[61], C. Talbot[16], A. J. Tanasijczuk[88], D. B. Tanner[41], D. Tao[11], M. Tápai[148], A. Tapia[38], E. N. Tapia San Martin[47], J. D. Tasson[209], R. Taylor[11], R. Tenorio[114], L. Terkowski[123], M. P. Thirugnanasambandam[13], M. Thomas[17], P. Thomas[57], J. E. Thompson[118], S. R. Thondapu[73], K. A. Thorne[17], E. Thrane[16], C. L. Tinsman[16], T. R. Saravanan[13], Shubhanshu Tiwari[84,130,131], S. Tiwari[152], V. Tiwari[118], K. Toland[61], M. Tonelli[31,65], Z. Tornasi[61], A. Torres-Forné[91], C. I. Torrie[11], I. Tosta e Melo[133,134], D. Töyrä[18], E. A. Trail[12], F. Travasso[51,66], G. Traylor[17], M. C. Tringali[89], A. Tripathee[154], A. Trovato[37], R. J. Trudeau[11], K. W. Tsang[47], M. Tse[62], R. Tso[58], L. Tsukada[97], D. Tsuna[97], T. Tsutsui[97], M. Turconi[80], A. S. Ubhi[23], K. Ueno[97], D. Ugolini[198], C. S. Unnikrishnan[152], A. L. Urban[12], S. A. Usman[106], A. C. Utina[61], H. Vahlbruch[20], G. Vajente[11], G. Valdes[12], M. Valentini[130,131], N. van Bakel[47], M. van Beuzekom[47], J. F. J. van den Brand[47,90,157], C. Van Den Broeck[47,210], D. C. Vander-Hyde[52], L. van der Schaaf[47], J. V. Van Heijningen[81], A. A. van Veggel[61], M. Vardaro[67,68], V. Varma[58], S. Vass[11], M. Vasúth[63], A. Vecchio[23], G. Vedovato[68], J. Veitch[61], P. J. Veitch[71], K. Venkateswara[179], G. Venugopalan[11], D. Verkindt[44], D. Veske[117], F. Vetrano[78,79], A. Viceré[78,79], A. D. Viets[211], S. Vinciguerra[23], D. J. Vine[75], J.-Y. Vinet[80], S. Vitale[62], Francisco Hernandez Vivanco[16], T. Vo[52], H. Vocca[50,51], C. Vorvick[57], S. P. Vyatchanin[74], A. R. Wade[18], L. E. Wade[193], M. Wade[193], R. Walet[47], M. Walker[38], G. S. Wallace[34], L. Wallace[11], S. Walsh[33], J. Z. Wang[154], S. Wang[30], W. H. Wang[26], R. L. Ward[18], Z. A. Warden[45], J. Warner[57], M. Was[44], J. Watchi[115], B. Weaver[57], L.-W. Wei[19,20], M. Weinert[19,20], A. J. Weinstein[11], R. Weiss[62], F. Wellmann[19,20], L. Wen[81], P. Weßels[19,20], J. W. Westhouse[45], K. Wette[18], J. T. Whelan[76], B. F. Whiting[41], C. Whittle[62], D. M. Wilken[19,20], D. Williams[61], J. L. Willis[11], B. Willke[19,20], W. Winkler[19,20], C. C. Wipf[11], H. Wittel[19,20], G. Woan[61], J. Woehler[19,20], J. K. Wofford[76], C. Wong[107], J. L. Wright[61], D. S. Wu[19,20], D. M. Wysocki[76], L. Xiao[11], H. Yamamoto[11], L. Yang[140], Y. Yang[41], Z. Yang[54], M. J. Yap[18], M. Yazback[41], D. W. Yeeles[118], Hang Yu[62], Haocun Yu[62], S. H. R. Yuen[107], A. K. Zadrożny[26], A. Zadrożny[170], M. Zanolin[45], T. Zelenova[40], J.-P. Zendri[68], M. Zevin[24], J. Zhang[81], L. Zhang[11], T. Zhang[61], C. Zhao[81], G. Zhao[115], M. Zhou[24], Z. Zhou[24], X. J. Zhu[16], A. B. Zimmerman[185], M. E. Zucker[11,62], and J. Zweizig[11]

The LIGO Scientific Collaboration and the Virgo Collaboration

[1] Department of Space Science, University of Alabama in Huntsville, Huntsville, AL 35899, USA
[2] Center for Space Plasma and Aeronomic Research, University of Alabama in Huntsville, Huntsville, AL 35899, USA
[3] Science and Technology Institute, Universities Space Research Association, Huntsville, AL 35805, USA
[4] NASA Goddard Space Flight Center, Greenbelt, MD 20771, USA
[5] Dipartimento Interateneo di Fisica, Politecnico di Bari, Via G. Amendola 126, I-70126, Bari, Italy

[6] Istituto Nazionale di Fisica Nucleare (INFN) Sezione di Bari, Via E. Orabona 4, I-70125, Bari, Italy
[7] Jacobs Space Exploration Group, Huntsville, AL 35806, USA
[8] NASA Marshall Space Flight Center, Huntsville, AL 35812, USA
[9] Max-Planck-Institut für extraterrestrische Physik, Giessenbachstrasse 1, D-85748 Garching, Germany
[10] NASA Marshall Space Flight Center, Huntsville, AL 35805, USA
[11] LIGO, California Institute of Technology, Pasadena, CA 91125, USA
[12] Louisiana State University, Baton Rouge, LA 70803, USA
[13] Inter-University Centre for Astronomy and Astrophysics, Pune 411007, India
[14] Dipartimento di Farmacia, Università di Salerno, I-84084 Fisciano, Salerno, Italy
[15] INFN, Sezione di Napoli, Complesso Universitario di Monte S.Angelo, I-80126 Napoli, Italy
[16] OzGrav, School of Physics & Astronomy, Monash University, Clayton 3800, Victoria, Australia
[17] LIGO Livingston Observatory, Livingston, LA 70754, USA
[18] OzGrav, Australian National University, Canberra, Australian Capital Territory 0200, Australia
[19] Max Planck Institute for Gravitational Physics (Albert Einstein Institute), D-30167 Hannover, Germany
[20] Leibniz Universität Hannover, D-30167 Hannover, Germany
[21] Theoretisch-Physikalisches Institut, Friedrich-Schiller-Universität Jena, D-07743 Jena, Germany
[22] University of Cambridge, Cambridge CB2 1TN, UK
[23] University of Birmingham, Birmingham B15 2TT, UK
[24] Center for Interdisciplinary Exploration & Research in Astrophysics (CIERA), Northwestern University, Evanston, IL 60208, USA
[25] Instituto Nacional de Pesquisas Espaciais, 12227-010 São José dos Campos, São Paulo, Brazil
[26] The University of Texas Rio Grande Valley, Brownsville, TX 78520, USA
[27] Gran Sasso Science Institute (GSSI), I-67100 L'Aquila, Italy
[28] INFN, Laboratori Nazionali del Gran Sasso, I-67100 Assergi, Italy
[29] International Centre for Theoretical Sciences, Tata Institute of Fundamental Research, Bengaluru 560089, India
[30] NCSA, University of Illinois at Urbana-Champaign, Urbana, IL 61801, USA
[31] INFN, Sezione di Pisa, I-56127 Pisa, Italy
[32] Laboratoire des Matériaux Avancés (LMA), IP2I—UMR 5822, CNRS, Université de Lyon, F-69622 Villeurbanne, France
[33] University of Wisconsin-Milwaukee, Milwaukee, WI 53201, USA
[34] SUPA, University of Strathclyde, Glasgow G1 1XQ, UK
[35] Dipartimento di Matematica e Informatica, Università di Udine, I-33100 Udine, Italy
[36] INFN, Sezione di Trieste, I-34127 Trieste, Italy
[37] APC, AstroParticule et Cosmologie, Université Paris Diderot, CNRS/IN2P3, CEA/Irfu, Observatoire de Paris, Sorbonne Paris Cité, F-75205 Paris Cedex 13, France
[38] California State University Fullerton, Fullerton, CA 92831, USA
[39] LAL, Univ. Paris-Sud, CNRS/IN2P3, Université Paris-Saclay, F-91898 Orsay, France
[40] European Gravitational Observatory (EGO), I-56021 Cascina, Pisa, Italy
[41] University of Florida, Gainesville, FL 32611, USA
[42] INFN, Sezione di Roma Tor Vergata, I-00133 Roma, Italy
[43] INFN, Sezione di Roma, I-00185 Roma, Italy
[44] Laboratoire d'Annecy de Physique des Particules (LAPP), Univ. Grenoble Alpes, Université Savoie Mont Blanc, CNRS/IN2P3, F-74941 Annecy, France
[45] Embry-Riddle Aeronautical University, Prescott, AZ 86301, USA
[46] Montclair State University, Montclair, NJ 07043, USA
[47] Nikhef, Science Park 105, 1098 XG Amsterdam, The Netherlands
[48] Korea Institute of Science and Technology Information, Daejeon 34141, Republic of Korea
[49] Christopher Newport University, Newport News, VA 23606, USA
[50] Università di Perugia, I-06123 Perugia, Italy
[51] INFN, Sezione di Perugia, I-06123 Perugia, Italy
[52] Syracuse University, Syracuse, NY 13244, USA
[53] Université de Liège, B-4000 Liège, Belgium
[54] University of Minnesota, Minneapolis, MN 55455, USA
[55] Università degli Studi di Milano-Bicocca, I-20126 Milano, Italy
[56] INFN, Sezione di Milano-Bicocca, I-20126 Milano, Italy
[57] LIGO Hanford Observatory, Richland, WA 99352, USA
[58] Caltech CaRT, Pasadena, CA 91125, USA
[59] Departament de Física Quàntica i Astrofísica, Institut de Ciències del Cosmos (ICCUB), Universitat de Barcelona (IEEC-UB), E-08028 Barcelona, Spain
[60] Dipartimento di Medicina, Chirurgia e Odontoiatria "Scuola Medica Salernitana," Università di Salerno, I-84081 Baronissi, Salerno, Italy
[61] SUPA, University of Glasgow, Glasgow G12 8QQ, UK
[62] LIGO, Massachusetts Institute of Technology, Cambridge, MA 02139, USA
[63] Wigner RCP, RMKI, H-1121 Budapest, Konkoly Thege Miklós út 29-33, Hungary
[64] Stanford University, Stanford, CA 94305, USA
[65] Università di Pisa, I-56127 Pisa, Italy
[66] Università di Camerino, Dipartimento di Fisica, I-62032 Camerino, Italy
[67] Università di Padova, Dipartimento di Fisica e Astronomia, I-35131 Padova, Italy
[68] INFN, Sezione di Padova, I-35131 Padova, Italy
[69] Montana State University, Bozeman, MT 59717, USA
[70] Nicolaus Copernicus Astronomical Center, Polish Academy of Sciences, 00-716, Warsaw, Poland
[71] OzGrav, University of Adelaide, Adelaide, South Australia 5005, Australia
[72] INFN, Sezione di Genova, I-16146 Genova, Italy
[73] RRCAT, Indore, Madhya Pradesh 452013, India
[74] Faculty of Physics, Lomonosov Moscow State University, Moscow 119991, Russia
[75] SUPA, University of the West of Scotland, Paisley PA1 2BE, UK
[76] Rochester Institute of Technology, Rochester, NY 14623, USA
[77] Bar-Ilan University, Ramat Gan 5290002, Israel
[78] Università degli Studi di Urbino "Carlo Bo," I-61029 Urbino, Italy
[79] INFN, Sezione di Firenze, I-50019 Sesto Fiorentino, Firenze, Italy
[80] Artemis, Université Côte d'Azur, Observatoire Côte d'Azur, CNRS, CS 34229, F-06304 Nice Cedex 4, France

4

[81] OzGrav, University of Western Australia, Crawley, Western Australia 6009, Australia
[82] Dipartimento di Fisica "E.R. Caianiello," Università di Salerno, I-84084 Fisciano, Salerno, Italy
[83] INFN, Sezione di Napoli, Gruppo Collegato di Salerno, Complesso Universitario di Monte S. Angelo, I-80126 Napoli, Italy
[84] Physik-Institut, University of Zurich, Winterthurerstrasse 190, 8057 Zurich, Switzerland
[85] Univ Rennes, CNRS, Institut FOTON—UMR6082, F-3500 Rennes, France
[86] University of Oregon, Eugene, OR 97403, USA
[87] Laboratoire Kastler Brossel, Sorbonne Université, CNRS, ENS-Université PSL, Collège de France, F-75005 Paris, France
[88] Université catholique de Louvain, B-1348 Louvain-la-Neuve, Belgium
[89] Astronomical Observatory Warsaw University, 00-478 Warsaw, Poland
[90] VU University Amsterdam, 1081 HV Amsterdam, The Netherlands
[91] Max Planck Institute for Gravitational Physics (Albert Einstein Institute), D-14476 Potsdam-Golm, Germany
[92] University of Maryland, College Park, MD 20742, USA
[93] School of Physics, Georgia Institute of Technology, Atlanta, GA 30332, USA
[94] Université de Lyon, Université Claude Bernard Lyon 1, CNRS, Institut Lumière Matière, F-69622 Villeurbanne, France
[95] Università di Napoli "Federico II," Complesso Universitario di Monte S.Angelo, I-80126 Napoli, Italy
[96] Dipartimento di Fisica, Università degli Studi di Genova, I-16146 Genova, Italy
[97] RESCEU, University of Tokyo, Tokyo, 113-0033, Japan
[98] Tsinghua University, Beijing 100084, People's Republic of China
[99] Texas Tech University, Lubbock, TX 79409, USA
[100] Università di Roma Tor Vergata, I-00133 Roma, Italy
[101] Missouri University of Science and Technology, Rolla, MO 65409, USA
[102] Departamento de Astronomía y Astrofísica, Universitat de València, E-46100 Burjassot, València, Spain
[103] Museo Storico della Fisica e Centro Studi e Ricerche "Enrico Fermi," I-00184 Roma, Italy
[104] National Tsing Hua University, Hsinchu City, 30013 Taiwan, People's Republic of China
[105] Charles Sturt University, Wagga Wagga, New South Wales 2678, Australia
[106] University of Chicago, Chicago, IL 60637, USA
[107] The Chinese University of Hong Kong, Shatin, NT, Hong Kong
[108] Dipartimento di Ingegneria Industriale (DIIN), Università di Salerno, I-84084 Fisciano, Salerno, Italy
[109] Institut de Physique des 2 Infinis de Lyon (IP2I)—UMR 5822, Université de Lyon, Université Claude Bernard, CNRS, F-69622 Villeurbanne, France
[110] Seoul National University, Seoul 08826, Republic of Korea
[111] Pusan National University, Busan 46241, Republic of Korea
[112] INAF, Osservatorio Astronomico di Padova, I-35122 Padova, Italy
[113] OzGrav, University of Melbourne, Parkville, Victoria 3010, Australia
[114] Universitat de les Illes Balears, IAC3—IEEC, E-07122 Palma de Mallorca, Spain
[115] Université Libre de Bruxelles, Brussels 1050, Belgium
[116] Departamento de Matemáticas, Universitat de València, E-46100 Burjassot, València, Spain
[117] Columbia University, New York, NY 10027, USA
[118] Cardiff University, Cardiff CF24 3AA, UK
[119] University of Rhode Island, Kingston, RI 02881, USA
[120] Bellevue College, Bellevue, WA 98007, USA
[121] MTA-ELTE Astrophysics Research Group, Institute of Physics, Eötvös University, Budapest 1117, Hungary
[122] California State University, Los Angeles, 5151 State University Drive, Los Angeles, CA 90032, USA
[123] Universität Hamburg, D-22761 Hamburg, Germany
[124] Institute for Plasma Research, Bhat, Gandhinagar 382428, India
[125] IGFAE, Campus Sur, Universidade de Santiago de Compostela, E-15782, Spain
[126] The University of Sheffield, Sheffield S10 2TN, UK
[127] Dipartimento di Scienze Matematiche, Fisiche e Informatiche, Università di Parma, I-43124 Parma, Italy
[128] INFN, Sezione di Milano Bicocca, Gruppo Collegato di Parma, I-43124 Parma, Italy
[129] Dipartimento di Ingegneria, Università del Sannio, I-82100 Benevento, Italy
[130] Università di Trento, Dipartimento di Fisica, I-38123 Povo, Trento, Italy
[131] INFN, Trento Institute for Fundamental Physics and Applications, I-38123 Povo, Trento, Italy
[132] Università di Roma "La Sapienza," I-00185 Roma, Italy
[133] Università degli Studi di Sassari, I-07100 Sassari, Italy
[134] INFN, Laboratori Nazionali del Sud, I-95125 Catania, Italy
[135] University of Portsmouth, Portsmouth, PO1 3FX, UK
[136] West Virginia University, Morgantown, WV 26506, USA
[137] The Pennsylvania State University, University Park, PA 16802, USA
[138] Physics and Astronomy Department, Stony Brook University, Stony Brook, NY 11794, USA
[139] Center for Computational Astrophysics, Flatiron Institute, 162 5th Avenue, New York, NY 10010, USA
[140] Colorado State University, Fort Collins, CO 80523, USA
[141] Institute for Nuclear Research (Atomki), Hungarian Academy of Sciences, Bem tér 18/c, H-4026 Debrecen, Hungary
[142] CNR-SPIN, c/o Università di Salerno, I-84084 Fisciano, Salerno, Italy
[143] Scuola di Ingegneria, Università della Basilicata, I-85100 Potenza, Italy
[144] National Astronomical Observatory of Japan, 2-21-1 Osawa, Mitaka, Tokyo 181-8588, Japan
[145] Observatori Astronòmic, Universitat de València, E-46980 Paterna, València, Spain
[146] INFN Sezione di Torino, I-10125 Torino, Italy
[147] Indian Institute of Technology Bombay, Powai, Mumbai 400 076, India
[148] University of Szeged, Dóm tér 9, Szeged 6720, Hungary
[149] Delta Institute for Theoretical Physics, Science Park 904, 1090 GL Amsterdam, The Netherlands
[150] Lorentz Institute, Leiden University, P.O. Box 9506, Leiden 2300 RA, The Netherlands
[151] GRAPPA, Anton Pannekoek Institute for Astronomy and Institute for High-Energy Physics, University of Amsterdam, Science Park 904, 1098 XH Amsterdam, The Netherlands
[152] Tata Institute of Fundamental Research, Mumbai 400005, India
[153] INAF, Osservatorio Astronomico di Capodimonte, I-80131 Napoli, Italy
[154] University of Michigan, Ann Arbor, MI 48109, USA
[155] American University, Washington, D.C. 20016, USA

[156] University of California, Berkeley, CA 94720, USA
[157] Maastricht University, P.O. Box 616, 6200 MD Maastricht, The Netherlands
[158] Directorate of Construction, Services & Estate Management, Mumbai 400094 India
[159] University of Białystok, 15-424 Białystok, Poland
[160] King's College London, University of London, London WC2R 2LS, UK
[161] University of Southampton, Southampton SO17 1BJ, UK
[162] University of Washington Bothell, Bothell, WA 98011, USA
[163] Institute of Applied Physics, Nizhny Novgorod, 603950, Russia
[164] Ewha Womans University, Seoul 03760, Republic of Korea
[165] Inje University Gimhae, South Gyeongsang 50834, Republic of Korea
[166] National Institute for Mathematical Sciences, Daejeon 34047, Republic of Korea
[167] Ulsan National Institute of Science and Technology, Ulsan 44919, Republic of Korea
[168] Bard College, 30 Campus Road, Annandale-On-Hudson, NY 12504, USA
[169] Chennai Mathematical Institute, Chennai 603103, India
[170] NCBJ, 05-400 Świerk-Otwock, Poland
[171] Institute of Mathematics, Polish Academy of Sciences, 00656 Warsaw, Poland
[172] Cornell University, Ithaca, NY 14850, USA
[173] Université de Montréal/Polytechnique, Montreal, Quebec H3T 1J4, Canada
[174] Lagrange, Université Côte d'Azur, Observatoire Côte d'Azur, CNRS, CS 34229, F-06304 Nice Cedex 4, France
[175] Hillsdale College, Hillsdale, MI 49242, USA
[176] Korea Astronomy and Space Science Institute, Daejeon 34055, Republic of Korea
[177] Institute for High-Energy Physics, University of Amsterdam, Science Park 904, 1098 XH Amsterdam, The Netherlands
[178] NASA Marshall Space Flight Center, Huntsville, AL 35811, USA
[179] University of Washington, Seattle, WA 98195, USA
[180] Dipartimento di Matematica e Fisica, Università degli Studi Roma Tre, I-00146 Roma, Italy
[181] INFN, Sezione di Roma Tre, I-00146 Roma, Italy
[182] ESPCI, CNRS, F-75005 Paris, France
[183] Center for Phononics and Thermal Energy Science, School of Physics Science and Engineering, Tongji University, 200092 Shanghai, People's Republic of China
[184] Southern University and A&M College, Baton Rouge, LA 70813, USA
[185] Department of Physics, University of Texas, Austin, TX 78712, USA
[186] Dipartimento di Fisica, Università di Trieste, I-34127 Trieste, Italy
[187] Centre Scientifique de Monaco, 8 quai Antoine Ier, MC-98000, Monaco
[188] Indian Institute of Technology Madras, Chennai 600036, India
[189] Université de Strasbourg, CNRS, IPHC UMR 7178, F-67000 Strasbourg, France
[190] Institut des Hautes Etudes Scientifiques, F-91440 Bures-sur-Yvette, France
[191] IISER-Kolkata, Mohanpur, West Bengal 741252, India
[192] Department of Astrophysics/IMAPP, Radboud University Nijmegen, P.O. Box 9010, 6500 GL Nijmegen, The Netherlands
[193] Kenyon College, Gambier, OH 43022, USA
[194] Whitman College, 345 Boyer Avenue, Walla Walla, WA 99362, USA
[195] Hobart and William Smith Colleges, Geneva, NY 14456, USA
[196] Department of Physics, Lancaster University, Lancaster, LA1 4YB, UK
[197] OzGrav, Swinburne University of Technology, Hawthorn VIC 3122, Australia
[198] Trinity University, San Antonio, TX 78212, USA
[199] Dipartimento di Fisica, Università degli Studi di Torino, I-10125 Torino, Italy
[200] Indian Institute of Technology, Gandhinagar Ahmedabad Gujarat 382424, India
[201] INAF, Osservatorio Astronomico di Brera sede di Merate, I-23807 Merate, Lecco, Italy
[202] Centro de Astrofísica e Gravitação (CENTRA), Departamento de Física, Instituto Superior Técnico, Universidade de Lisboa, 1049-001 Lisboa, Portugal
[203] Marquette University, 11420 W. Clybourn Street, Milwaukee, WI 53233, USA
[204] Indian Institute of Technology Hyderabad, Sangareddy, Khandi, Telangana 502285, India
[205] INAF, Osservatorio di Astrofisica e Scienza dello Spazio, I-40129 Bologna, Italy
[206] International Institute of Physics, Universidade Federal do Rio Grande do Norte, Natal RN 59078-970, Brazil
[207] Villanova University, 800 Lancaster Avenue, Villanova, PA 19085, USA
[208] Andrews University, Berrien Springs, MI 49104, USA
[209] Carleton College, Northfield, MN 55057, USA
[210] Department of Physics, Utrecht University, 3584CC Utrecht, The Netherlands
[211] Concordia University Wisconsin, 2800 N Lake Shore Drive, Mequon, WI 53097, USA

Abstract

We present results from offline searches of Fermi Gamma-ray Burst Monitor (GBM) data for gamma-ray transients coincident with the compact binary coalescences observed by the gravitational-wave (GW) detectors Advanced LIGO and Advanced Virgo during their first and second observing runs. In particular, we perform follow-up for both confirmed events and low significance candidates reported in the LIGO/Virgo catalog GWTC-1. We search for temporal coincidences between these GW signals and GBM-triggered gamma-ray bursts (GRBs). We also use the GBM Untargeted and Targeted subthreshold searches to find coincident gamma-rays below the onboard triggering threshold. This work implements a refined statistical approach by incorporating GW astrophysical source probabilities and GBM visibilities of LIGO/Virgo sky localizations to search for cumulative signatures of coincident subthreshold gamma-rays. All search methods recover the short gamma-ray burst GRB 170817A occurring ∼1.7 s after the binary neutron-star merger GW170817. We also present results from a new search seeking GBM counterparts to LIGO single-interferometer triggers. This search finds a candidate joint event, but

---

[212] NASA Postdoctoral Fellow.

given the nature of the GBM signal and localization, as well as the high joint false alarm rate of 1.1×10^{-6} Hz, we do not consider it an astrophysical association. We find no additional coincidences.

Unified Astronomy Thesaurus concepts: Gamma-ray bursts (629); Gravitational waves (678)

1. Introduction

Simultaneous observations of the same source in gravitational waves (GWs) and gamma-rays probe some of the most cataclysmic events in the universe and create rich opportunities to study fundamental physics, cosmology, and high energy astrophysics. This was demonstrated by the joint observations (Abbott et al. 2017d) of the binary neutron-star (BNS) coalescence GW170817 (Abbott et al. 2019b, 2017e) and the short gamma-ray burst GRB 170817A (Goldstein et al. 2017; Savchenko et al. 2017). These observations led to constraints on the speed of gravity (Abbott et al. 2017a), an independent measure of the Hubble constant (Abbott et al. 2019a, 2017b; Hotokezaka et al. 2019), evidence for heavy element production via *r*-process nucleosynthesis in a kilonova (e.g., Chornock et al. 2017; Cowperthwaite et al. 2017; Kasen et al. 2017; Tanvir et al. 2017; Watson et al. 2019), and more. Motivated by the wealth of science gained from multimessenger observations such as these, we seek to increase the number of joint GW/gamma-ray detections by performing coordinated analysis of candidates from Advanced LIGO (Aasi et al. 2015), Advanced Virgo (Acernese et al. 2015), and the Fermi Gamma-ray Burst Monitor (GBM; Meegan et al. 2009).

The first LIGO/Virgo science observing run (O1) ran from 2015 September to 2016 January, during which GBM performed online analyses of GW candidates from compact binary coalescence (CBC) searches. For GBM offline analysis (Burns et al. 2019), trigger selection was conservative, treating all CBC candidates with a false alarm rate (FAR) of less than 10^{-5} Hz (about 1/day) as equally plausible for follow-up. The CBC candidates were used to search for coincidences with GBM-triggered GRBs and subthreshold short GRBs from the offline Untargeted Search (M. S. Briggs et al. 2020, in preparation). CBC event times were also used to seed more sensitive follow-up with the Targeted Search (Blackburn et al. 2015) of GBM data. No unambiguous coincidences were found between the GBM and LIGO/Virgo candidates. The most significant event found in the GBM follow-up search was associated with the first observed binary black hole (BBH) coalescence, GW150914 (Abbott et al. 2016b). However the GBM candidate, GW150914-GBM, could not be unambiguously claimed as an electromagnetic counterpart due to its extremely weak signal and poor localization (Connaughton et al. 2016; Greiner et al. 2016; Connaughton et al. 2018).

For the second observing run (O2), running from 2016 November to 2017 August, the GBM Targeted Search was improved (Goldstein et al. 2016) and run autonomously, in low latency, again following up CBC triggers with FAR $< 10^{-5}$ Hz. The most interesting multimessenger event from O2 was the association between GW170817 and GRB 170817A. The Targeted Search proved redundant in this case, as the GRB produced a trigger on board Fermi.[213] However, had the source been ~10 Mpc farther from Earth, it would not have triggered the detectors on board GBM and would have only been detectable with subthreshold searches

(Abbott et al. 2017d; Goldstein et al. 2017), while still being well within the LIGO/Virgo detection horizon (Abbott et al. 2017e).

In this work, we perform an offline follow-up of all CBC triggers published in the first LIGO/Virgo gravitational-wave transient catalog (GWTC-1; Abbott et al. 2019c). Our search methods are akin to LIGO/Virgo searches for GWs coincident with GRBs (Abbott et al. 2017c, 2019d). In addition to seeking coincidences to individual GW events, we search on a statistical basis, looking for any cumulative effects that subthreshold gamma-ray counterparts might have on the resulting follow-up distribution. We improve upon the GBM analysis of O1 triggers in Burns et al. (2019), in that the joint association calculation no longer treats all CBC candidates equally. Instead, the analysis accounts for the astrophysical nature of the CBC candidates as well as their potential visibility with respect to GBM. This is done by incorporating the probability that each CBC candidate originated from an astrophysical rather than terrestrial source and also considering the fraction of LIGO/Virgo localization probability that was observable to GBM at GW trigger time. Finally, we augment GBM follow-up of GW events by also reporting results from a new search method (Stachie et al. 2020) that seeks gamma-rays coincident with LIGO single-interferometer triggers.

This paper is organized as follows. In Section 2, we describe the sample of gravitational-wave candidates and the GBM searches used to follow-up this sample. Section 3 summarizes the results of these searches, including the search for coincidences with single-interferometer triggers, and discusses the probability of association between the GW and gamma-ray candidate events. In Section 4, we conclude and discuss future prospects for GBM follow-up of GWs.

2. Method

2.1. Gravitational-wave Trigger Selection

The Advanced LIGO (Aasi et al. 2015) and Virgo (Acernese et al. 2015) observatories are kilometer-scale Michelson laser interferometers designed to detect GWs. Multiple search pipelines are used to detect CBC events in strain data, with each pipeline making different assumptions about the signals and the detector noise and using different technical solutions to maximize detection efficiency. We focus on events generated by two pipelines: PyCBC (Usman et al. 2016) and GstLAL (Messick et al. 2017). Both rely on accurate physical models of the gravitational waveform radiated by a CBC event and use the models to perform matched filtering on strain data. The process of matched filtering produces a signal-to-noise ratio (S/N) over a large number of templates covering the CBC parameter space. The extent of the parameter space chosen for O2 and the method used to construct the template bank are described for PyCBC and GstLAL in Dal Canton & Harry (2017) and Mukherjee et al. (2018), respectively. Once the S/N has been calculated over all templates, S/N-peaks above a certain threshold are recorded as single-detector CBC triggers. Non-Gaussian and nonstationary detector noise fRequently

---

[213] https://gcn.gsfc.nasa.gov/other/524666471.fermi

Table 1
Gravitational-wave Triggers from Abbott et al. (2019c)

LIGO/Virgo				GBM
GW Event	UTC Date	UTC Time	p_{astro}	Coverage
GW150914	2015 Sep 14	09:50:45.4	1	66.7%
151008	2015 Oct 8	14:09:17.5	0.27	100%
151012.2	2015 Oct 12	06:30:45.2	0.023	58.4%
GW151012	2015 Oct 12	09:54:43.4	1	66.1%
151116	2015 Nov 16	22:41:48.7	≪0.5	72.6%
GW151226	2015 Dec 26	03:38:53.6	1	78.8%
161202	2016 Dec 2	03:53:44.9	0.034	⋯
161217	2016 Dec 17	07:16:24.4	0.018	⋯
GW170104	2017 Jan 4	10:11:58.6	1	90.3%
170208	2017 Feb 8	10:39:25.8	0.02	97.8%
170219	2017 Feb 19	14:04:09.0	0.02	5.1%
170405	2017 Apr 5	11:04:52.7	0.004	⋯
170412	2017 Apr 12	15:56:39.0	0.06	67.2%
170423	2017 Apr 23	12:10:45.0	0.086	45.2%
GW170608	2017 Jun 8	02:01:16.5	1	73.0%
170616	2017 Jun 16	19:47:20.8	≪0.5	66.2%
170630	2017 Jun 30	16:17:07.8	0.02	8.2%
170705	2017 Jul 5	08:45:16.3	0.012	26.3%
170720	2017 Jul 20	22:44:31.8	0.0097	48.2%
GW170729	2017 Jul 29	18:56:29.3	0.98	88.9%
GW170809	2017 Aug 9	08:28:21.8	1	73.9%
GW170814	2017 Aug 14	10:30:43.5	1	73.6%
GW170817	2017 Aug 17	12:41:04.4	1	100%
GW170818	2017 Aug 18	02:25:09.1	1	100%
GW170823	2017 Aug 23	13:13:58.5	1	⋯

Note. The p_{astro} values shown here are the maximum values reported between the GstLAL and PyCBC pipelines. The percentage of the LIGO/Virgo localization probability that was visible to GBM at trigger time is also given. Triggers with unspecified coverage are due to GBM passage through the South Atlantic Anomaly when all detectors are turned off.

produces nonastrophysical triggers with large S/N, hence the pipelines employ a variety of techniques to veto or down-rank such triggers. The surviving triggers are used in a coincidence analysis, and each pair of triggers occurring within the maximum GW travel time between detectors produces a coincident trigger. The coincident trigger is assigned a ranking statistic that takes into account (i) S/N in the GW detectors, (ii) signal-based vetoes indicating the compatibility of the waveform with a CBC signal, and (iii) the probability of the observed combination of S/N, time delay, and phase difference at the different detectors to be produced by an astrophysical signal (e.g., Nitz et al. 2017). The final step is mapping the coincident rank to a statistical significance, which in the case of CBC pipelines is reported via two different quantities: the FAR of the search at the time of the trigger and the probability that the trigger has an astrophysical origin (p_{astro}; Kapadia et al. 2020). p_{astro} is estimated using our current understanding of the population of real signals weighed against the distribution of background (false signals) due to GW detector noise fluctuations.

We perform GBM follow-up of all 25 CBC triggers reported in the LIGO/Virgo catalog GWTC-1 (Abbott et al. 2019c). This catalog utilized state-of-the-art configurations of PyCBC and GstLAL, as well as the best data-quality selection of the LIGO and Virgo strain data available, for a full reanalysis of O1 and O2. Listed in Table 1, the catalog triggers were required to pass an initial threshold of FAR ≲ 3.86 × 10⁻⁷ Hz (about 1/30 days) in at least one pipeline. Triggers passing this

FAR threshold and additionally having p_{astro} greater than 50% are denoted with "GW" in the event name. In the follow-up analyses, the GBM searches are guided by the CBC trigger times. To assess GBM coverage of the LIGO/Virgo triggers, the public HEALPix (Górski et al. 2005) sky localization maps accompanying GWTC-1 are taken for the high p_{astro} detections (LIGO Scientific & Virgo Collaboration 2019). We generate BAYESTAR skymaps (Singer & Price 2016) for all remaining triggers which had corresponding GBM data. BAYESTAR skymaps rely on the mass and spin parameters reported by the searches and do not marginalize over them, as is done instead for high p_{astro} detections via full parameter estimation (Veitch et al. 2015; Abbott et al. 2016a). Nevertheless, they allow approximations of GBM observing coverages at much lower computational costs. Finally, for each CBC trigger, the maximum p_{astro} is used between the GstLAL and PyCBC pipelines (Abbott et al. 2019c, Table IV).

2.2. Fermi-GBM Searches

GBM is a survey instrument on board the Fermi Gamma-ray Space Telescope and is comprised of 14 scintillation detectors that span an energy range of 8 keV–40 MeV (Meegan et al. 2009). Twelve of the detectors are made of thallium-doped sodium iodide (NaI) crystals and are oriented in such a manner as to cover the entire sky unocculted by the Earth (∼70%). The two other detectors are bismuth germanate (BGO) crystals positioned on opposite sides of the spacecraft. Triggering algorithms running on the satellite search data on multiple timescales and energy ranges for coherent, statistically significant (usually 4σ) excesses in at least 2 NaI detectors (Bhat et al. 2016; von Kienlin et al. 2020). Localization is performed by combining the detector responses with a set of three template photon spectra representing spectrally hard, normal, and soft GRBs to generate expected photon counts from points evenly spaced across a 1° grid of the sky (Connaughton et al. 2015). The expected count rates are compared to the observed rates, and a χ^2 minimization process identifies the most likely direction, with localization accuracy on the order of degrees. GBM continuously takes data except during passage through the South Atlantic Anomaly (SAA) when the detectors are turned off due to high particle flux, yielding an uptime of approximately 85%.

GBM has developed increased sensitivity to weak, short GRBs by means of two offline searches: the Untargeted Search[214] (M. S. Briggs et al. 2020, in preparation) and the Targeted Search (Blackburn et al. 2015; Goldstein et al. 2016). These searches seek transient signals that do not exceed the high threshold set by the onboard triggering algorithms, and in this work, they are employed to find subthreshold gamma-rays coincident with the GW triggers in our search sample. Additional details on these searches follow.

2.2.1. Untargeted Search

The Untargeted Search is a blind search of continuous time-tagged event (CTTE) data, running automatically upon receipt of data from the Fermi spacecraft and using no information from GW searches. The search improves upon the onboard triggering algorithms by utilizing additional energy ranges and timescales, as well as a more sophisticated background-fitting

---

[214] https://gcn.gsfc.nasa.gov/fermi_gbm_subthresh_archive.html

model. Candidate events are required to have excess counts greater than 2.5σ relative to background in one detector and at least 1.25σ in a second detector. Significant candidates are autonomously distributed via the Gamma-ray Coordinates Network along with HEALPix skymaps to facilitate joint detections with other instruments (see, e.g., Zhang et al. 2017). Further details on the Untargeted Search and an analysis of its candidates will be published in a forthcoming article.

2.2.2. Targeted Search

The Targeted Search was designed for multimessenger follow-up, requiring an input time and/or HEALPix skymap to seed a sensitive search of CTTE data. When seeking counterparts to GWs, the Targeted Search analyzes a 60 s window centered on the input GW time and searches timescales increasing by powers of 2 from 64 ms to 8.192 s, while phasing time bins by a factor of 4. Data from all 14 detectors are processed coherently to achieve a greater sensitivity to weak signals than when analyzing one detector at a time, as performed by the onboard flight software and the Untargeted Search. Three model spectra, described in Goldstein et al. (2016), are folded through the detector responses to produce templates of expected counts which are then compared to the observed distribution of counts in each energy channel of each detector. The comparison is performed via a log-likelihood ratio (Λ), testing the alternative hypothesis of the presence of a signal with a similar spectrum versus the null hypothesis of only background noise. Treating Λ as our detection statistic, the model spectrum resulting in the highest Λ is selected as the preferred spectrum, and this procedure is repeated for each bin of data in the search (see Blackburn et al. 2015 for the detailed calculation of Λ). Bins contaminated by phosphorescent noise events are removed, and overlapping bins are merged to produce only the most significant bin. After this filtering, all remaining bins are retained as candidate events for our analysis. The different spectral templates tend to identify different types of sources in the GBM background, and such types may have very different rates of occurrence. To preserve sensitivity to these different sources, the bins are separated by best-fit spectral template, and event significance (i.e., FAR) is measured against background from the same template.

The Targeted Search was made more sensitive in preparation for O2 by improving the background estimation, revising the spectral template for hard GRBs, and implementing additional automated filters (Goldstein et al. 2016). In particular, a Λ prefilter was applied. The Λ calculation demands an initial estimation of the signal amplitude (effectively, the photon fluence in the time bin over 50–300 keV) that maximizes the likelihood of the hypothesis that a signal exists. The prefilter excludes time bins with initial guesses of $\Lambda < 5$ from the full numerical optimization, increasing the speed of this computationally expensive task by up to a factor of 5. Bins with $\Lambda < 5$ have been verified to lie well within the GBM background, thus excluding them does not affect the sensitivity of the search. This updated version of the Targeted Search was used to analyze both the O1 and O2 triggers in our sample. Further improvements have been made for online analysis of CBC triggers during Advanced LIGO and Advanced Virgo's third observing run (Goldstein et al. 2019), but were not used in this work.
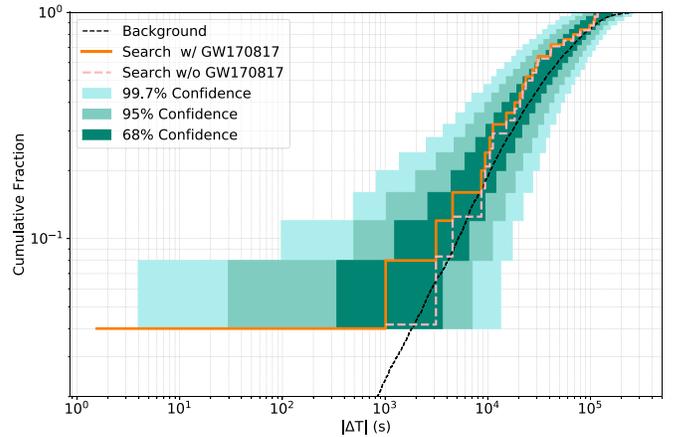

Figure 1. Cumulative distribution for the minimal time offsets between the 25 CBC triggers and GRBs found by either the GBM onboard triggering algorithms or the Untargeted Search. The background offset distribution is shown in black. The search sample including GW170817 is depicted by the solid gold line, and the search excluding GW170817 is shown by the dashed brown line.

3. Results

Here we present the results of our searches for gamma-ray counterparts to the GW triggers in our sample. To quantify event significance, each resulting search distribution is compared to that of background. The background used in the following sections is composed of randomly selected times during which both LIGO detectors were in observing mode during O1 and O2. The ratio of random background between O1 and O2 is also roughly proportional to the LIGO/Virgo livetimes during O1 and O2. The same Targeted Search input parameters used for the search sample were used for the background, resulting in $\sim$10 (20) ks of background during O1 (O2), yielding a minimum FAR of $\sim$1 $\times$ 10^{-5} ($\sim$5 $\times$ 10^{-6}) Hz for Targeted Search analysis. Finally, the background times were chosen independently with respect to GBM and therefore include GBM trigger times.

3.1. GBM Trigger and Untargeted Search Results

As done in Burns et al. (2019), we first examine the time offsets between the search sample of CBC triggers and both GRBs detected by the GBM onboard flight software and subthreshold short GRB candidates from the Untargeted Search. This method is similar to the RAVEN analysis used by LIGO/Virgo (Urban 2016). The Untargeted Search sample consists of all 187 candidates published during O1 and O2 via GCN, as described in the previous section. Combining these with the triggered GRBs, we obtained a total of 474 GRBs. The temporal offsets between the 25 GW events and the GBM GRBs were then determined, and the smallest offset for each GW candidate was taken. The search sample offsets are compared to those arising from random coincidences by finding the shortest temporal offsets between the background times and the GW trigger times. Both positive and negative offsets were allowed for search sample and background, but a maximum offset was not enforced. GW triggers occurring during Fermi passage through SAA were included, limiting the minimum time offsets for some GBM events; however, the same treatment for the search was used for background.

The cumulative distribution for this search is presented in Figure 1. The search sample including GW170817 is shown
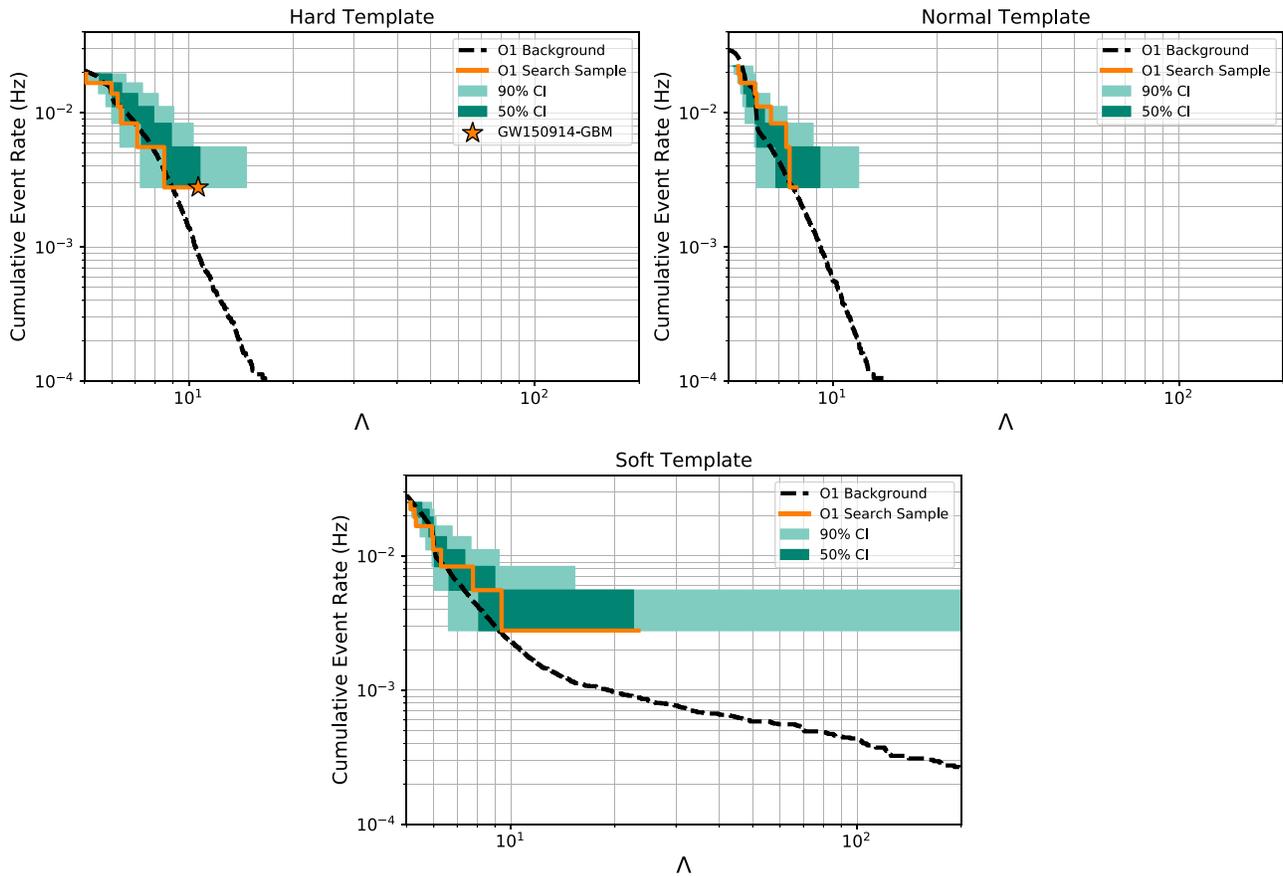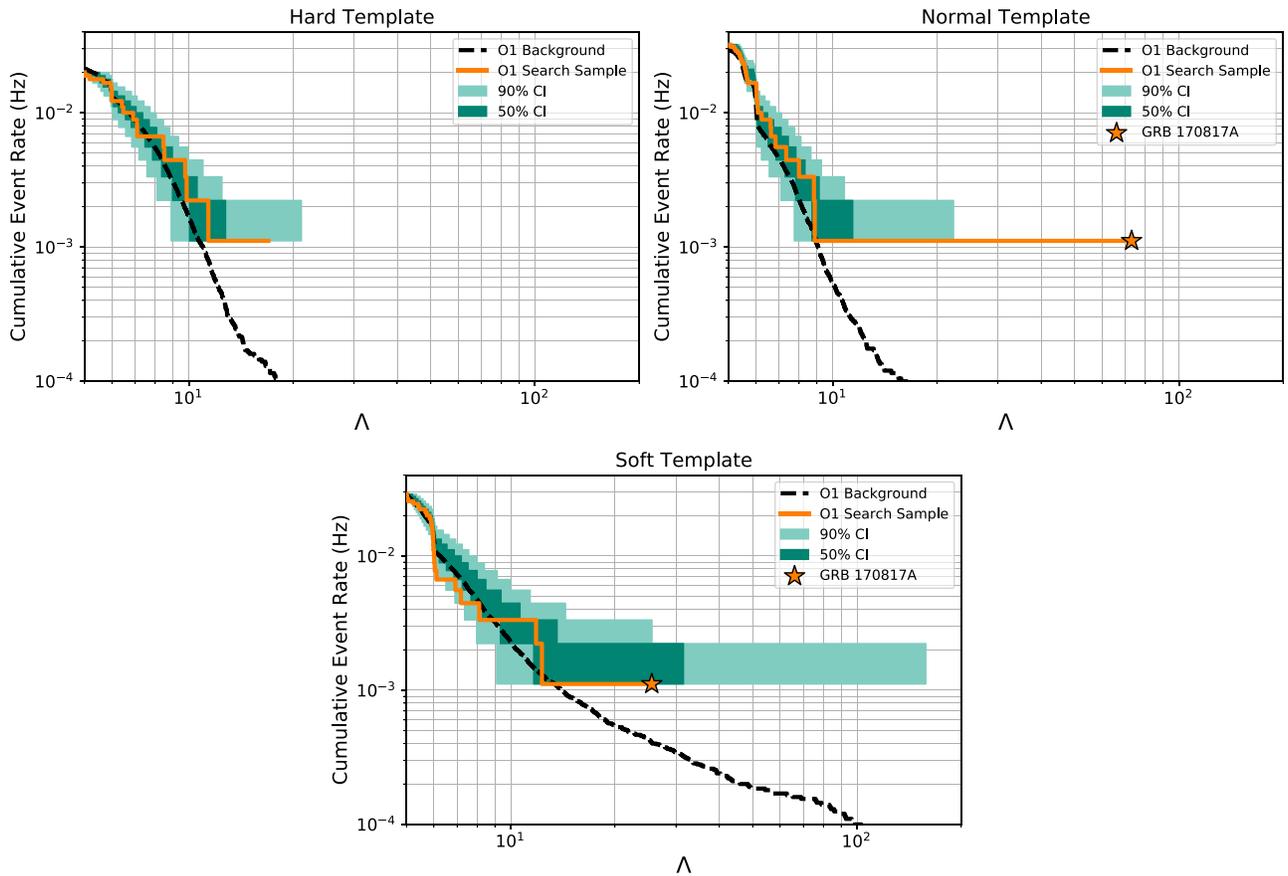
9

Figure 2. O1 cumulative event rate distributions of the GBM background (black dashed lines) and search samples (solid gold line) for the GBM Targeted Search as a function of the log-likelihood ratio. Distributions are separated according to best-fitting spectral template. The transient GW150914-GBM is marked by a gold star in the hard template distribution.

with the solid gold line, while the distribution without GW170817 is displayed by the dashed brown line. Confidence regions were obtained empirically by Monte Carlo sampling of the background offset distribution with sample size equal to that of the search sample and finding the desired percentiles. The most significant deviation of the search distribution from that of random background is caused by GRB 170817A, found ~ 1.7 s after GW170817. Omitting GW170817, the shortest time interval between a CBC trigger from our sample and a GBM event is approximately 1000 s. On-axis prompt emission from a short GRB is not expected at such large time delays after a BNS merger (Vedrenne & Atteia 2009; Zhang 2019), though larger delays may be allowed for off-axis emission (e.g., Salafia et al. 2018). Hence, with this first search we find no evidence for GW/gamma-ray associations apart from GW170817/GRB 170817A.

3.2. Targeted Search Results

The Targeted Search was used to search for subthreshold gamma-ray signals around 21 events from the CBC search sample. GBM data were not collected around triggers 161202, 161217, 170405, and GW170823 due to passage through the SAA; therefore, these events were excluded from this search. For those remaining, the GBM coverage of the LIGO/Virgo localizations (see Table 1) was obtained. No LIGO/Virgo skymap was fully occulted by the Earth, and GBM observed

between $\sim 5\%$ and 100% of the localization probability with an average observing fraction of 67.0%.

The Targeted Search follow-up distributions for O1 triggers and O2 triggers are shown as functions of Λ in Figures 2 and 3, respectively. The background distributions were constructed by running the Targeted Search over the randomly selected times described above with the same parameters used for the search sample. As described in the previous section, confidence intervals for the search samples were produced by Monte Carlo sampling the background Λ distributions with the same sample size as the search sample. The distributions are separated into three categories according to the best-fitting spectral template, due to the different backgrounds affecting the three templates. Also, because of the time-variable nature of the background in each template, we obtain event significance by comparing the follow-up of O1 triggers to GBM background taken during O1 and O2 follow-up to O2 background.

For both O1 and O2, the search distributions lie largely within the 90% confidence region of the median for all spectral templates. The O1 follow-up (Figure 2) does not show any significant outliers in the sample distributions. The transient GW150914-GBM is found with a FAR of 8.7×10^{-4} Hz in the hard template distribution, where the FAR is the cumulative event rate of the background at the same Λ, and lies just within 50% confidence. The most significant event in the O2 follow-up (Figure 3) can be seen in the normal template distribution and is GRB 170817A, found with a FAR of 2.0×10^{-5} Hz. The spectrally soft tail of GRB 170817A is also the most

Figure 3. O2 cumulative event rate distributions of the GBM background (black dashed lines) and search samples (solid gold line) for the GBM Targeted Search as a function of the log-likelihood ratio. Distributions are separated according to the best-fitting spectral template. Both the main peak and soft thermal tail of GRB 170817A, the short gamma-ray burst counterpart to GW170817, are indicated by gold stars in the normal and soft template distributions, respectively.

significant foreground event in the O2 soft template distribution, with a FAR of 4.1×10^{-4} Hz, but is within the 50% confidence region. No other significant candidates are found.

3.3. Targeted Search Joint Analysis

The FARs discussed in the previous section measure the significance of GBM transients with respect to the Targeted Search background only, regardless of the GW observations. Here we characterize the significance of coincidences between the GW events and the gamma-ray signals from the Targeted Search. In our previous works (e.g., Connaughton et al. 2016; Burns et al. 2019), this was done by ranking gamma-ray candidates by the Targeted Search FAR and the relative time offsets between the candidates and the GW triggers. We build upon these analyses by also considering (i) the probability that the GW signal is astrophysical in origin and (ii) the fraction of the LIGO/Virgo sky localization visible to GBM at the GW event time. Therefore, we rank gamma-ray candidates found by the Targeted Search with a statistic R defined as

$$R = \frac{p_{\mathrm{astro}} \times p_{\mathrm{visible}}}{|\Delta t| \times \mathrm{FAR}_{\mathrm{GBM}}}, \quad (1)$$

where Δt is the time offset between the GW trigger and the gamma-ray event and p_{visible} is the fraction of the LIGO/Virgo localization probability observable to GBM. A minimum offset of 64 ms was set to match the time binning of the data. GW triggers 151116 and 170616 were given the lowest p_{astro} of the

sample (i.e., 0.004) in light of the upper limits reported in GWTC-1 (see Table 1). Background events are ranked using the same statistic R. As background events have no corresponding LIGO/Virgo information, skymaps and p_{astro} values from the GW search sample were randomly assigned to each background event, and the fraction of GBM visibility was calculated at the background time using the randomly selected skymap.

The ranking statistic of the search sample is mapped to a p-value, defined as the number of more highly ranked background events divided by the total number of background events, or $p_i = N(R > R_i)/N$, where N is the number of gamma-ray events in the background and i is the index of an event in the search sample. Again, search sample events from O1 and O2 are compared to background from O1 and O2, respectively. The cumulative distributions of the combined O1 and O2 p-values are shown in Figure 4, with and without GW170817 follow-up. The dashed black lines follow a uniform distribution, representing the null hypothesis that the search sample is consistent with that of background. The confidence regions for the p-value distribution were generated by random sampling of the background uniform distribution with sample size equal to the search sample size.

For the search including GW170817 follow-up, excesses of greater than 3 σ are observed due to contributions from GRB 170817A. The main emission peak of GRB 170817A has a higher ranking than any other event in the background, making
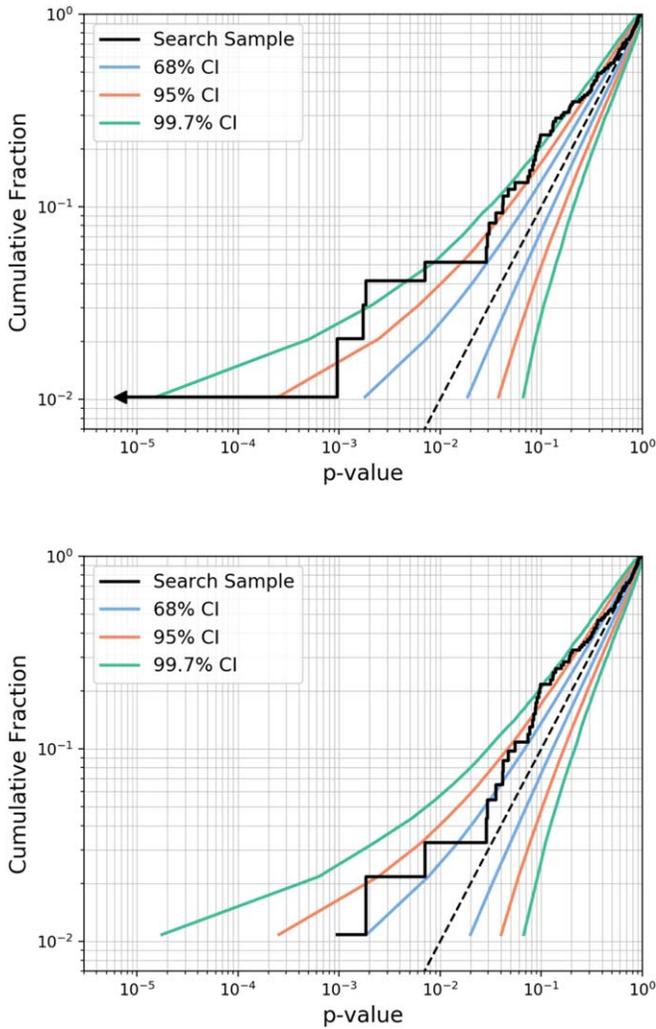
Figure 4. Cumulative distribution of the Targeted Search *p*-values. The dashed black lines represent the expected background distribution. Top: follow-up search sample including GW170817. The main emission episode of GRB 170817A is found with higher ranking than any other candidate within the background distribution. Its *p*-value is therefore marked as an upper limit (black triangle) at greater than 3σ deviation from the background *p*-value distribution. Bottom: follow-up search sample without GW170817.

its *p*-value an upper limit. Removing all Targeted Search candidates associated with GW170817, excesses greater than 2σ are still observed. Contributing to this near the tail of the distribution is GW150914-GMB, which is found with a *p*-value of $\sim 1.8 \times 10^{-3}$. Of the remaining candidates (located around *p*-value $= 1.0 \times 10^{-1}$), the detector lightcurves, spectral information, and localizations have been manually inspected. Real signals have consistent signal in detectors viewing approximately the same portion of the sky and are likely be found on multiple timescales by the Targeted Search. Short GRB-like signals typically display most of their emission above 50 keV. However, softer events with localizations consistent the Sun or the Galactic plane are likely to be solar flares or galactic sources rather than GRBs. All inspected events were judged to be either inconsistent with real short GRB-like signals or too weak in GBM data to constrain any properties. Therefore we judge this excess likely unrelated to the CBCs in the search sample. Some of the excess may be due to real but unrelated gamma-ray signals, and future observations can be used to either exclude or strengthen this feature.

We do not find evidence here to report any associations other than GW170817 and GRB 170817A.

3.4. Targeted Search Follow-up of Single Interferometer Triggers

During O1 and O2, a single LIGO interferometer taking science observing-mode data covered 33.4% and 29.5% of the respective livetimes. CBC events occurring during these times can still be detected (Callister et al. 2017; Sachdev et al. 2019), albeit with a reduced significance due to the lack of coincidence with a second detector. The lack of a second detector can be somewhat mitigated by searching for a coincident gamma-ray transient (Nitz et al. 2019) as the physical connection between GWs and GRBs has been established for at least BNS mergers. This idea is roughly illustrated by the narrative of GW170817, which was initially a single-interferometer trigger due to the presence of a glitch in the LIGO Livingston detector (Abbott et al. 2017e; Pankow et al. 2018), but was nonetheless found to be time-coincident with GRB 170817A.

The method for searching for GBM counterparts to single-interferometer triggers differs from those presented in the previous sections. We start from PyCBC single-interferometer triggers having a reweighted S/N (Usman et al. 2016) higher than 8, yielding a sample of 1621 (1126 for O2 and 495 for O1) triggers. The search for gamma-ray counterparts is then performed using the Targeted Search. We only consider possible associations between PyCBC candidates and the most significant GBM candidates found within the corresponding ± 30 s search windows. Thus, we obtain pairs of GW candidates and gamma-ray candidates and compute a joint statistical significance. This statistic is calculated by taking into account (i) the time offset, (ii) the reweighted S/N of the GW trigger, (iii) the Targeted Search Λ, and (iv) the overlap between the GW and gamma-ray sky localizations defined in Ashton et al. (2018). Further details on the statistical method will be given in Stachie et al. (2020). Although we find no highly significant associations, a close inspection of the data around the 80 candidates with the highest significance (i.e., lowest FAR) was performed. For these candidates, LIGO detector characterization was performed using standard tools like Omicron scans, Omega scans, and Used Percentage Veto (Isogai et al. 2010; Abbott et al. 2016c, 2018). Sixty-four candidates in temporal proximity with known types of instrumental transients, blip glitches (Abbott et al. 2016c; Cabero et al. 2019), nonstationary noise visible in spectrograms, and scattered light were rejected. There were 12 other triggers disfavored because parameter estimation (Veitch & Vecchio 2010) either showed evidence of a glitch (i.e., the existence of bimodality in posterior probability for different CBC parameters) or returned a low (<5) $\log_{10}$ Bayes factor. The Bayes factor compares the hypothesis of the presence of signal in the data to the hypothesis of the presence of Gaussian noise, with a low Bayes factor indicating the data contain little evidence of a signal. Three candidates were also eliminated due to noticeably poor background fits in the low-energy channels of the GBM detectors, which often cause inflated Λ values.

A single L1 surviving coincident association remained with no obvious reason for rejection. However, the derived FAR, based on coincidences between noises in LIGO and noises in GBM (Stachie et al. 2020), is relatively high at 1.1×10^{-6} Hz. The implied low significance is mainly due to the soft spectrum of the GBM candidate. The GBM candidate has a localization consistent with the galactic plane and is likely produced by

Scorpius X-1, as a strong occultation step caused by this Galactic X-ray source was observed close in time to the trigger. Finally, the parameter estimation of the LIGO signal indicates masses of $>100\ M_\odot$ for the two components of the binary. As of yet, there are no confirmed observations of such binary mergers (Abbott et al. 2019e), which suggests that these systems, if they exist, are not common.

4. Summary and Future Directions

We have used LIGO/Virgo and Fermi-GBM data and multiple algorithms to search for gamma-ray transients associated with high and low significance CBC events reported in the first gravitational-wave transient catalog, GWTC-1. The GBM subthreshold searches for gamma-ray candidates employed improved algorithms to conduct more sensitive searches than those used in online follow-up during O1 and O2. All searches identified the coincidence between the short gamma-ray burst GRB 170817A and the BNS coalescence signal GW170817. We found no additional coincident detections between CBC triggers and GBM triggers or Untargeted Search candidates. The GBM Targeted Search found the main emission peak and the long, soft tail of GRB 170817A with FARs of 2.0×10^{-5} Hz and 4.1×10^{-4} Hz, respectively, and the p-value of the joint association was found to deviate from the background distribution at greater than 3σ. The gamma-ray transient GW150914-GBM was also found with a FAR of 8.7×10^{-4} Hz, but was not a significant candidate on its own, lying just within the 50% confidence region of the hard spectral template. Future multimessenger observations will be necessary to establish any astrophysical connection between gamma-ray emission and BBH mergers (see, e.g., Veres et al. 2019). No other short GRB candidates were found in association with the CBC triggers.

In this work, the joint analysis was improved compared to that performed in Burns et al. (2019). In addition to the temporal offset and the Targeted Search FAR, we also considered the significance of the LIGO/Virgo trigger and the GBM visibility of the LIGO/Virgo sky localization. However, this analysis can be further refined. By including all candidates reported in GWTC-1, we implicitly assumed that BBH, BNS, and NSBH (i.e., neutron star-black hole) mergers are equally likely to produce gamma-ray emission, and sought counterparts to these mergers using a wide parameter space of different timescales, energy ranges, and spectral templates. The broad nature of this search was motivated by the fact that, with only one confirmed coincidence, the observational properties of joint GW/GRB events are still largely unknown. Improving our search to target short GRB-like signals and filter transients from sources unrelated to CBCs, such as particle and galactic flares, may increase sensitivity to coincident, subthreshold short GRBs. Improvements in GBM search pipelines (Goldstein et al. 2019) and formal methodology (e.g., Ashton et al. 2018) are being undertaken for joint LIGO/Virgo and GBM analysis of CBC triggers from O3.

Finally, a new search for GBM coincidences with LIGO single-interferometer triggers was also conducted. The most interesting resulting candidate is unlikely to be an astrophysical association because of its high FAR. Additionally, the gamma-ray signal was likely caused by flaring activity from a source near the Galactic plane and parameter estimation of the LIGO signal suggests source masses inconsistent with a neutron-star

coalescence. For future observing runs (Abbott et al. 2019f), the single-interferometer search methods will be improved. The introduction of several types of follow-up methods will be one of the modifications introduced during these subsequent runs. This will result in an improved FAR distribution, as future observations will assess associations between a specific category of CBC candidates (BNS, NSBH, or BBH) and GBM candidates defined by their duration and spectral hardness.

This research also made use of Astropy, a community-developed core Python package for Astronomy (Astropy Collaboration et al. 2013); NumPy (Van Der Walt et al. 2011); SciPy (Jones et al. 2001); and matplotlib, a Python library for publication quality graphics (Hunter 2007).

ORCID iDs

A. Goldstein ⬤ https://orcid.org/0000-0002-0587-7042
E. Bissaldi ⬤ https://orcid.org/0000-0001-9935-8106
C. Malacaria ⬤ https://orcid.org/0000-0002-0380-0041
S. Poolakkil ⬤ https://orcid.org/0000-0002-6269-0452
P. Veres ⬤ https://orcid.org/0000-0002-2149-9846
A. von Kienlin ⬤ https://orcid.org/0000-0002-0221-5916
C. A. Wilson-Hodge ⬤ https://orcid.org/0000-0002-8585-0084
K. Agatsuma ⬤ https://orcid.org/0000-0002-3952-5985
S. Banagiri ⬤ https://orcid.org/0000-0001-7852-7484
I. Bartos ⬤ https://orcid.org/0000-0001-5607-3637
C. Casentini ⬤ https://orcid.org/0000-0001-8100-0579
N. Cornish ⬤ https://orcid.org/0000-0002-7435-0869
A. Corsi ⬤ https://orcid.org/0000-0001-8104-3536
M. W. Coughlin ⬤ https://orcid.org/0000-0002-8262-2924
T. Dent ⬤ https://orcid.org/0000-0003-1354-7809
Z. Doctor ⬤ https://orcid.org/0000-0002-2077-4914
S. Fairhurst ⬤ https://orcid.org/0000-0001-8480-1961
W. M. Farr ⬤ https://orcid.org/0000-0003-1540-8562
M. Fishbach ⬤ https://orcid.org/0000-0002-1980-5293
T. J. Hansen ⬤ https://orcid.org/0000-0001-6154-8983
J. Heinze ⬤ https://orcid.org/0000-0003-4983-7672
A. M. Holgado ⬤ https://orcid.org/0000-0003-4143-8132
D. E. Holz ⬤ https://orcid.org/0000-0002-0175-5064
J. S. Key ⬤ https://orcid.org/0000-0003-0123-7600
P. Koch ⬤ https://orcid.org/0000-0003-2777-5861
M. Mapelli ⬤ https://orcid.org/0000-0001-8799-2548
B. J. Owen ⬤ https://orcid.org/0000-0003-3919-0780
C. Pankow ⬤ https://orcid.org/0000-0002-1128-3662
P. M. Ricker ⬤ https://orcid.org/0000-0002-5294-0630
Shubhanshu Tiwari ⬤ https://orcid.org/0000-0003-1611-6625
M. Valentini ⬤ https://orcid.org/0000-0003-0974-4148
D. Veske ⬤ https://orcid.org/0000-0003-4225-0895

References

Aasi, J., Abbott, R., Abbott, T., et al. 2015, CQGra, 32, 074001
Abbott, B., Abbott, R., Abbott, T., et al. 2016a, PhRvL, 116, 241102
Abbott, B., Abbott, R., Abbott, T., et al. 2018, CQGra, 35, 065010
Abbott, B. P., Abbott, R., Abbott, T., et al. 2017a, ApJL, 848, L13
Abbott, B. P., Abbott, R., Abbott, T. D., et al. 2016b, PhRvL, 116, 061102
Abbott, B. P., Abbott, R., Abbott, T. D., et al. 2016c, CQGra, 33, 134001
Abbott, B. P., Abbott, R., Abbott, T. D., et al. 2017b, Natur, 551, 85
Abbott, B. P., Abbott, R., Abbott, T. D., et al. 2017c, ApJ, 841, 89
Abbott, B. P., Abbott, R., Abbott, T. D., et al. 2017d, ApJL, 848, L12
Abbott, B. P., Abbott, R., Abbott, T. D., et al. 2017e, PhRvL, 119, 161101
Abbott, B. P., Abbott, R., Abbott, T. D., et al. 2019a, arXiv:1908.06060
Abbott, B. P., Abbott, R., Abbott, T. D., et al. 2019b, PhRvX, 9, 011001
Abbott, B. P., Abbott, R., Abbott, T. D., et al. 2019c, PhRvX, 9, 031040
Abbott, B. P., Abbott, R., Abbott, T. D., et al. 2019d, ApJ, 886, 75
Abbott, B. P., Abbott, R., Abbott, T. D., et al. 2019e, PhRvD, 100, 064064
Abbott, B. P., Abbott, R., Abbott, T. D., et al. 2019f, arXiv:1304.0670
Acernese, F., Agathos, M., Agatsuma, K., et al. 2015, CQGra, 32, 024001
Ashton, G., Burns, E., Dal Canton, T., et al. 2018, ApJ, 860, 6
Astropy Collaboration, Robitaille, T. P., Tollerud, E. J., et al. 2013, A&A, 558, A33
Bhat, P. N., Meegan, C. A., von Kienlin, A., et al. 2016, ApJS, 223, 28
Blackburn, L., Briggs, M. S., Camp, J., et al. 2015, ApJS, 217, 8
Burns, E., Goldstein, A., Hui, C. M., et al. 2019, ApJ, 871, 90
Cabero, M., Lundgren, A., Nitz, A. H., et al. 2019, CQGra, 36, 155010
Callister, T. A., Kanner, J. B., Massinger, T. J., Dhurandhar, S., & Weinstein, A. J. 2017, CQGra, 34, 155007
Chornock, R., Berger, E., Kasen, D., et al. 2017, ApJL, 848, L19
Connaughton, V., Briggs, M. S., Goldstein, A., et al. 2015, ApJS, 216, 32
Connaughton, V., Burns, E., Goldstein, A., et al. 2016, ApJL, 826, L6
Connaughton, V., Burns, E., Goldstein, A., et al. 2018, ApJL, 853, L9
Cowperthwaite, P. S., Berger, E., Villar, V. A., et al. 2017, ApJL, 848, L17
Dal Canton, T., & Harry, I. W. 2017, arXiv:1705.01845
Goldstein, A., Burns, E., & Hamburg, R. 2016, arXiv:1612.02395
Goldstein, A., Hamburg, R., Wood, J., et al. 2019, arXiv:1903.12597
Goldstein, A., Veres, P., Burns, E., et al. 2017, ApJL, 848, L14
Górski, K. M., Hivon, E., Banday, A. J., et al. 2005, ApJ, 622, 759
Greiner, J., Burgess, J. M., Savchenko, V., & Yu, H.-F. 2016, ApJL, 827, L38
Hotokezaka, K., Nakar, E., Gottlieb, O., et al. 2019, NatAs, 3, 940
Hunter, J. D. 2007, CSE, 9, 90
Isogai, T. & the Ligo Scientific Collaboration, & the Virgo Collaboration 2010, JPhCS, 243, 012005
Jones, E., Oliphant, T., Peterson, P., et al. 2001, SciPy: Open Source Scientific Tools for Python, http://www.scipy.org/
Kapadia, S. J., Caudill, S., Creighton, J. D. E., et al. 2020, CQGra, 37, 045007
Kasen, D., Metzger, B., Barnes, J., Quataert, E., & Ramirez-Ruiz, E. 2017, Natur, 551, 80
LIGO Scientific & Virgo Collaboration 2019, Sky Localization Probability Maps (skymaps) Release for GWTC-1, https://dcc.ligo.org/LIGO-P1800381/public
Meegan, C., Lichti, G., Bhat, P. N., et al. 2009, ApJ, 702, 791
Messick, C., Blackburn, K., Brady, P., et al. 2017, PhRvD, 95, 042001
Mukherjee, D., Caudill, S., Magee, R., et al. 2018, arXiv:1812.05121
Nitz, A. H., Dent, T., Dal Canton, T., Fairhurst, S., & Brown, D. A. 2017, ApJ, 849, 118
Nitz, A. H., Nielsen, A. B., & Capano, C. D. 2019, ApJL, 876, L4
Pankow, C., Chatziioannou, K., Chase, E. A., et al. 2018, PhRvD, 98, 084016
Sachdev, S., Caudill, S., Fong, H., et al. 2019, arXiv:1901.08580
Salafia, O. S., Ghisellini, G., Ghirlanda, G., & Colpi, M. 2018, A&A, 619, A18
Savchenko, V., Ferrigno, C., Kuulkers, E., et al. 2017, ApJL, 848, L15
Singer, L. P., & Price, L. R. 2016, PhRvD, 93, 024013
Stachie, C., Canton, T. D., Burns, E., et al. 2020, arXiv:2001.01462
Tanvir, N. R., Levan, A. J., González-Fernández, C., et al. 2017, ApJL, 848, L27
Urban, A. L. 2016, PhD thesis, Univ. Wisconsin Milwaukee
Usman, S. A., Nitz, A. H., Harry, I. W., et al. 2016, CQGra, 33, 215004
Van Der Walt, S., Colbert, S. C., & Varoquaux, G. 2011, CSE, 13, 22
Vedrenne, G., & Atteia, J.-L. 2009, Gamma-Ray Bursts: The Brightest Explosions in the Universe (Berlin: Springer), 385
Veitch, J., Raymond, V., Farr, B., et al. 2015, PhRvD, 91, 042003
Veitch, J., & Vecchio, A. 2010, PhRvD, 81, 062003
Veres, P., Dal Canton, T., Burns, E., et al. 2019, ApJ, 882, 53
von Kienlin, A., Meegan, C. A., & Paciesas, W. S. 2020, ApJ, 893, 46
Watson, D., Hansen, C. J., Selsing, J., et al. 2019, Natur, 574, 497
Zhang, B. 2019, FrPhy, 14, 64402
Zhang, Y. F., Xiong, S. L., Liao, J. Y., et al. 2017, GCN, 21919, 1